Two-peaked and flat-top perfect bright solitons in nonlinear metamaterials with epsilon near zero

C. Rizza,[1] A. Ciattoni,[2,3,*] and E. Palange[1]

[1]*Dipartimento di Ingegneria Elettrica e dell'Informazione, Università dell'Aquila, I-67100 Monteluco di Roio, L'Aquila, Italy*

[2]*Consiglio Nazionale delle Ricerche, CNR-SPIN 67100 L'Aquila, Italy*

[3]*Dipartimento di Fisica, Università dell'Aquila, 67100 Coppito, L'Aquila, Italy*

(Received 17 November 2010; published 5 May 2011)

We investigate analytically transverse-magnetic spatial bright solitons, as exact solutions of Maxwell's equations, propagating through nonlinear metamaterials whose linear dielectric permittivity is very close to zero and whose effective nonlinear Kerr parameters can be tailored to achieve values not available in standard materials. Exploiting the fact that, in the medium considered, linear and nonlinear polarization can be comparable at feasible and realistic optical intensities, we identify two self-trapping mechanisms able to support two-peaked and flat-top solitons, respectively. Specifically, these two mechanisms are based on the occurrence of critical points at which the effective nonlinear permittivity vanishes, the two mechanisms differing in the way the compensation between linear and nonlinear polarization is achieved through the nonstandard values of the nonlinear parameters.

DOI: 10.1103/PhysRevA.83.053805 PACS number(s): 42.65.Tg, 78.67.Pt

I. INTRODUCTION

Metamaterials have recently attracted a great deal of attention since they are characterized by unconventional electromagnetic properties and suggest alternative and fascinating applications [1–5]. In the context of nonlinear optics, metamaterials offer two different ways to overcome its fundamental limit consisting in the fact that, due to the weakness of the nonlinear response, nonlinear behavior is observed at large optical intensities. In the first scheme the material is tailored in such a way that the nonlinear medium is placed in the region where a large field enhancement occurs [6,7], whereas in the second scheme the linear dielectric permittivity is chosen to be so small as to allow the nonlinear polarization to fully rule the electromagnetic behavior (extreme nonlinear regime) [8]. Such an extreme nonlinear regime has recently been used to predict genuinely different and intriguing phenomena such as beam transverse power flow reversing [9] where the Poynting vector flips its sign along the transverse profile of an optical beam since optical radiation nonlinearly produces a region (around the beam propagation axis) where the dielectric behaves as a metal. A nonlinear slab characterized by a very small optical intensity has been shown to support transmissivity directional hysteresis [10] and the corresponding underlying electromagnetic multiplicity has been shown to be produced by the nonlinear field matching at the slab interfaces in the extreme nonlinear regime. In the context of nondiffracting and self-trapped waves, nonlinear epsilon-near-zero metamaterials have recently been shown to be able to support dark solitons characterized by a central and extended region where the Poynting vector vanishes exactly together with the transverse electric-field component [11].

In this paper we investigate analytically transverse-magnetic (TM) spatial bright solitons propagating through epsilon-near-zero nonlinear Kerr metamaterials (material proposed in Ref. [8]) and we predict the existence of two perfect soliton [12] families whose Poynting vector profiles are two peaked and flat top [13,14], respectively. Such metamaterials host the extreme nonlinear regime where, due to the small value of the linear dielectric permittivity, linear and nonlinear polarizations can be comparable at feasible optical intensities. As a consequence, critical electromagnetic points are allowed where the overall effective nonlinear permittivity vanishes. In this work we prove that these points can be profitably exploited to tailor the soliton shape, allowing us to obtain both two-peaked and flat-top solitons. The occurrence of such points provides different physical self-trapping mechanisms (much more involved than the standard compensation between self-focusing and diffraction) where the longitudinal electric-field component (i.e., the component parallel to the soliton propagation direction) is the basic mean to produce the above-mentioned balance between linear and nonlinear polarizations. The full exploitation of such self-trapping mechanisms is possible since the nonlinear parameters of the metamaterial Kerr response (as discussed in Ref. [8]) can be tailored to assume values not available in standard materials. In order to prove the feasibility of the two soliton families, we propose a realistic composite medium characterized by a sufficient number of parameters that can be independently tuned to allow the overall homogenized medium response to meet the conditions required for observing both two-peaked and flat-top solitons. In addition, as a consequence of the small value of the linear permittivity, two-peaked and flat-top solitons turn out to be observable at feasible optical intensities.

The paper is organized as follow. In Sec. II we discuss epsilon-near-zero nonlinear metamaterials, we introduce the basic theory for investigating bright solitons, and we derive their existence conditions even for values of the nonlinear parameters not available in nature but available through the proposed nonlinear metamaterial. In Secs. III and IV we consider two-peaked and flat-top solitons, respectively, and we focus on their underlying self-trapping supporting mechanisms by discussing their mutual differences and the role played by the unconventional values of the nonlinear parameters. In Sec. V we propose a feasible and realistic composite medium (nonlinear metamaterial) suitable for observing two-peaked and flat-top solitons. Finally, in Sec. VI we conclude with a discussion and summary of our results.

*alessandro.ciattoni@aquila.infn.it

II. BRIGHT SOLITONS IN NONLINEAR EPSILON-NEAR-ZERO METAMATERIALS

Consider monochromatic TM fields $\mathbf{E} = \mathrm{Re}[\mathbf{E}\exp(-i\omega t)]$ and $\mathbf{H} = \mathrm{Re}[\mathbf{H}\exp(-i\omega t)]$ (of frequency ω), where

$$\begin{aligned}\mathbf{E} &= E_x(x,z)\hat{\mathbf{e}}_x + E_z(x,z)\hat{\mathbf{e}}_z,\\ \mathbf{H} &= H_y(x,z)\hat{\mathbf{e}}_y,\end{aligned} \tag{1}$$

propagating through a nonlinear metamaterial whose effective medium response is described by the constitutive relations

$$\begin{aligned}\mathbf{D} &= \epsilon_0\epsilon\mathbf{E} + \epsilon_0\chi[|\mathbf{E}|^2\mathbf{E} + \gamma(\mathbf{E}\cdot\mathbf{E})\mathbf{E}^*],\\ \mathbf{B} &= \mu_0\mu\mathbf{H},\end{aligned} \tag{2}$$

where ϵ and μ are the linear dielectric permittivity and magnetic permeability, respectively, and χ and γ are parameters characterizing the overall effective nonlinear Kerr response. As opposed to conventional media where $\epsilon \geqslant 1$, $\mu \simeq 1$, and γ assumes three values depending on the physical mechanism supporting the Kerr nonlinear response [15] (i.e., $\gamma = 0$ for electrostriction, $\gamma = 0.5$ for the nonresonant electronic response, and $\gamma = 3$ for molecular orientation), we focus hereinafter on suitable metamaterials designed to exhibit a very small dielectric permittivity $|\epsilon| \ll 1$ [16], an arbitrary μ, and with γ attaining, in principle, any real value. The possibility of tailoring both linear and nonlinear medium responses has been investigated in the pioneering work of Ref. [17] in which Sipe and Boyd consider a composite structure comprised of spherical inclusion particles embedded in a host material. Remarkably, if the inclusions respond linearly and the host material responds nonlinearly, the composite is characterized by a nonlinear effective Kerr response whose parameter γ spans the range $0 < \gamma < 3$ [17]. Recently, we [8] improved these results by showing that TM optical waves traveling through a nonlinear layered medium, in the long-wavelength limit, experience a nonlinear optical response described by Eqs. (2) whose electromagnetic parameters can be independently tailored. In particular, using positive and negative (linear and nonlinear) dielectric layers, we have shown that a suitable composite tailoring allows γ to achieve any prescribed value (even encompassing negative values) and ϵ, at the same time, to assume a value very close to zero. The evident consequence of operating with a very small dielectric permittivity is that the extreme nonlinear regime can be observed where the nonlinear polarization can be comparable with the linear part [8], i.e., the condition

$$\chi[|\mathbf{E}|^2\mathbf{E} + \gamma(\mathbf{E}\cdot\mathbf{E})\mathbf{E}^*] \approx \epsilon\mathbf{E} \tag{3}$$

can be satisfied at small and feasible optical intensities. Note that in standard media where $\epsilon \approx 1$, the condition of Eq. (3) is strictly meaningless since the Kerr nonlinearity is always a perturbation to the linear polarization and, for very high intensities, it always displays a form of saturation, thus departing from the cubic behavior and never reaching values of the order of $\epsilon\mathbf{E}$. Therefore, even though Eqs. (2) formally coincide with the standard nonlinear Kerr response, the media considered host a marked and hitherto unexplored nonlinear behavior (extreme nonlinear regime) accessible at feasible optical intensities. It is worth stressing that, since the very small value of the permittivity is achieved herein by averaging negative and positive dielectric permittivities, it is evident that suitable gain media have to be inserted among the underlying medium constituents in order to compensate for losses due to the presence of negative dielectrics (see Sec. V).

We focus on nondiffracting solitary waves propagating along the z axis of the kind

$$\begin{aligned}E_x &= \sqrt{|\epsilon/\chi|}\,u_x(\xi)\exp(i\beta\zeta),\\ E_z &= i\sqrt{|\epsilon/\chi|}\,u_z(\xi)\exp(i\beta\zeta),\end{aligned} \tag{4}$$

where $\xi = \sqrt{|\mu\epsilon|}k_0x$, $\zeta = \sqrt{|\mu\epsilon|}k_0z$ (dimensionless spatial coordinates), $k_0 = \omega/c$, and we require β (the dimensionless propagation constant) and u_x and u_z (the dimensionless field amplitudes) to be real quantities. Note that, using dimensionless field amplitudes introduced through Eqs. (4), the extreme nonlinear regime condition of Eq. (3) can be stated as

$$\begin{aligned}u_x^2 &\approx 1,\\ u_z^2 &\approx 1.\end{aligned} \tag{5}$$

Maxwell equations $\nabla\times\mathbf{E} = i\omega\mathbf{B}$ and $\nabla\times\mathbf{H} = -i\omega\mathbf{D}$ for the fields of Eqs. (1) and (4) and with the constitutive relations of Eqs. (2) yield, after some algebra, the system of first-order differential equations

$$\begin{aligned}\beta\frac{du_z}{d\xi} &= \left(\beta^2 - \sigma_\mu\epsilon_x^{\mathrm{NL}}\right)u_x,\\ \beta\frac{du_x}{d\xi} &= \frac{\beta^2\epsilon_z^{\mathrm{NL}}u_z - \left(\beta^2 - \sigma_\mu\epsilon_x^{\mathrm{NL}}\right)\frac{\partial\epsilon_x^{\mathrm{NL}}}{\partial u_z}u_x^2}{\epsilon_x^{\mathrm{NL}} + \frac{\partial\epsilon_x^{\mathrm{NL}}}{\partial u_x}u_x},\end{aligned} \tag{6}$$

where $\sigma_\epsilon = \epsilon\chi/|\epsilon\chi|$, $\sigma_\mu = \mu\chi/|\mu\chi|$, and we have defined

$$\begin{aligned}\epsilon_x^{\mathrm{NL}} &= \sigma_\epsilon + (1+\gamma)u_x^2 + (1-\gamma)u_z^2,\\ \epsilon_z^{\mathrm{NL}} &= \sigma_\epsilon + (1-\gamma)u_x^2 + (1+\gamma)u_z^2\end{aligned} \tag{7}$$

as effective normalized nonlinear dielectric permittivities. We note that the system of equations in Eqs. (6) is equivalent to Maxwell's equations if the condition

$$\epsilon_x^{\mathrm{NL}} + \frac{\partial\epsilon_x^{\mathrm{NL}}}{\partial u_x}u_x \neq 0 \tag{8}$$

holds along the whole field profile. It is worth stressing that the system of equations in Eqs. (6) is integrable since it admits the first integral

$$\begin{aligned}F(u_x,u_z) = {}& \left[(\beta^2 - \sigma_\epsilon\sigma_\mu)u_x^2 - \sigma_\epsilon\sigma_\mu u_z^2\right]\\ & - \frac{1}{2}\sigma_\mu(1+\gamma)\left(u_x^4 + u_z^4\right) - \sigma_\mu(1-\gamma)u_x^2u_z^2\\ & - \frac{1}{\beta^2}\left\{(\beta^2 - \sigma_\epsilon\sigma_\mu) - \sigma_\mu\left[(1+\gamma)u_x^2\right.\right.\\ & \left.\left. + (1-\gamma)u_z^2\right]\right\}^2u_x^2,\end{aligned} \tag{9}$$

i.e., the relation $dF/d\xi = 0$ is satisfied along the solutions $u_x(\xi)$ and $u_z(\xi)$ of Eqs. (6) (see Ref. [8] for details). Here we investigate bright solitons whose normalized electric-field components u_x and u_z asymptotically vanish at infinity and are spatially even $[u_x(\xi) = u_x(-\xi)]$ and odd $[u_z(\xi) = -u_z(-\xi)]$, so that we consider the boundary conditions $u_x(0) = u_{x0}$, $u_z(0) = 0$, $u_x(+\infty) = 0$, and $u_z(+\infty) = 0$. The vanishing of

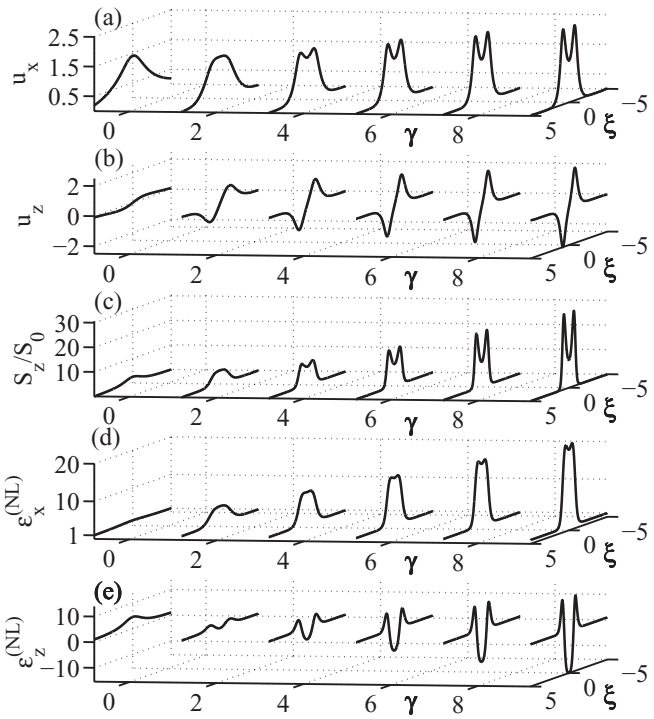

FIG. 1. Profiles of (a) $u_x(\xi)$, (b) $u_z(\xi)$, and (c) the normalized Poynting vector $S_z(\xi)/S_0$ of various bright solitons with $\sigma_\epsilon = 1$, $\sigma_\mu = 1$, $\mathrm{sgn}(\chi) = 1$, $u_{x0}^2 = 2$, and γ spanning the range $-0.8 < \gamma < 10$. Also shown are the effective normalized nonlinear dielectric permittivities (d) $\epsilon_x^{\mathrm{NL}}(\xi)$ and (e) $\epsilon_z^{\mathrm{NL}}(\xi)$ of Eqs. (7) evaluated for the profiles of $u_x(\xi)$ [from (a)] and $u_z(\xi)$ [from (b)].

the field at infinity implies that the first integral F has to vanish along the whole soliton profile, i.e., $F[u_x(\xi),u_z(\xi)] = 0$, a relation that, evaluated at $\xi = 0$, allows us to evaluate analytically the propagation constant

$$\beta^2 = 2\sigma_\mu \frac{\left[\sigma_\epsilon + (1+\gamma)u_{x0}^2\right]^2}{2\sigma_\epsilon + 3(1+\gamma)u_{x0}^2}. \tag{10}$$

Remarkably, bright solitons are represented in the phase space (u_x,u_z) by the special level curves $F(u_x,u_z) = 0$, which are orbits of the dynamical system of equations in Eqs. (6) (known as homoclinic orbits) joining the equilibrium point $(u_x,u_z) = (0,0)$ to itself. The main consequence of this identification is that bright solitons asymptotically coincide for $\xi \to \pm\infty$ with the linear inhomogeneous transverse plane waves $e^{\mp\sqrt{\beta^2-\sigma_\epsilon\sigma_\mu}\xi}$, respectively, so that the relation

$$\beta^2 - \sigma_\epsilon\sigma_\mu > 0 \tag{11}$$

is a necessary condition for soliton existence. The existence of at least one turning point (i.e., where $du_z/d\xi = 0$ occurs) along the orbit corresponding to a bright soliton is an additional condition to be met, which is fulfilled by requiring the curves $F(u_x,u_z) = 0$ and $(\beta^2 - \sigma_\mu\epsilon_x^{\mathrm{NL}})u_x = 0$ [see the first of Eqs. (6)] to have an intersection. These necessary conditions for the existence of bright solitons, together with Eq. (8), allow us to obtain the results of Table I, where we report, for each possible combination of σ_ϵ and σ_μ, the range of u_{x0}^2 (depending on γ) where bright solitons can be excited.

TABLE I. Bright soliton existence ranges of u_{x0}^2 depending on γ, σ_ϵ, and σ_μ. The parameter α is defined in Eq. (14).

γ	$\sigma_\epsilon = 1,\sigma_\mu = 1$	$\sigma_\epsilon = -1,\sigma_\mu = -1$
> -1	$\forall u_{x0}^2$	
< -1		$u_{x0}^2 < \alpha(\gamma)$

III. TWO-PEAKED SOLITONS

A first group of bright solitons (see Table I) exists for any values of u_{x0}^2 in the range $\gamma > -1$ and for $\sigma_\epsilon = 1$ and $\sigma_\mu = 1$ (i.e., for right-handed metamaterials with focusing nonlinearity $\chi > 0$ or for left-handed metamaterials with defocusing nonlinearity $\chi < 0$). Note that this group of bright solitons encompasses the perfect optical solitons described in Ref. [12], where only the standard Kerr nonlinearity arising from the electronic nonresonant response ($\gamma = 0.5$) was considered. In Figs. 1(a) and 1(b) we report the bright soliton profiles of u_x and u_z, respectively, for $u_{x0}^2 = 2$, $-0.8 < \gamma < 10$, $\sigma_\epsilon = 1$, and $\sigma_\mu = 1$. For completeness, in Fig. 1(c) we report the profiles of the normalized Poynting vector $S_z(\xi)/S_0 = \mathrm{sgn}(\mu)[(\beta u_x - du_z/d\xi)u_x]\hat{\mathbf{e}}_z$ (where $S_0 = \sqrt{\epsilon_0|\epsilon|^3/4\mu_0|\mu|\chi^2}$) corresponding to the solitons reported in Figs. 1(a) and 1(b). In addition, in Figs. 1(d) and 1(e) we report the effective normalized nonlinear dielectric permittivities $\epsilon_x^{\mathrm{NL}}(\xi)$ and $\epsilon_z^{\mathrm{NL}}(\xi)$ of Eqs. (7) evaluated for the profiles of $u_x(\xi)$ and $u_z(\xi)$ of Figs. 1(a) and 1(b). From Fig. 1 we note that two-peaked bright solitons can be excited, i.e., solitons whose electric-field x components and Poynting vectors show two pronounced peaks along their transverse profiles; the higher the value of γ the more pronounced the two peaks are. From Figs. 1(d) and 1(e) it is worth noting that in the region where the soliton Poynting vector displays the two-peaked structure, the overall normalized dielectric permittivities $\epsilon_x^{\mathrm{NL}}(\xi)$ and $\epsilon_z^{\mathrm{NL}}(\xi)$ are generally much greater than their asymptotic linear values [i.e., $\epsilon_x^{\mathrm{NL}}(\infty) = \epsilon_z^{\mathrm{NL}}(\infty) = \sigma_\epsilon = 1$] so the solitons considered can be observed only in the extreme nonlinear regime where the nonlinear contribution to the medium polarization can be much greater than the linear one.

In order to grasp the underlying mechanism producing such an atypical (for the Kerr nonlinearity) two-peaked soliton profile, we consider the equilibrium points of the system of equations in Eqs. (6) [i.e., $du_x/d\xi = 0$ and $du_z/d\xi = 0$, hence necessarily coinciding with the critical points of the first integral $F(u_x,u_z)$], which, in addition to the origin $(u_x,u_z) = (0,0)$, are given by the relations

$$\begin{aligned} &\beta^2 - \sigma_\mu\epsilon_x^{\mathrm{NL}} = 0, \\ &\epsilon_z^{\mathrm{NL}}u_z = 0. \end{aligned} \tag{12}$$

Note that the number of critical points of F depends, in addition to u_{x0}^2, on the value of the nonlinear parameter γ. In fact, for $|\gamma| < 1$ [see Fig. 2(a)] F has only a maximum at the point $(u_x,u_z) = [\sqrt{(\beta^2-1)/(1+\gamma)},0]$ (belonging to the axis $u_z = 0$) and a saddle point at the origin $(u_x,u_z) = (0,0)$;

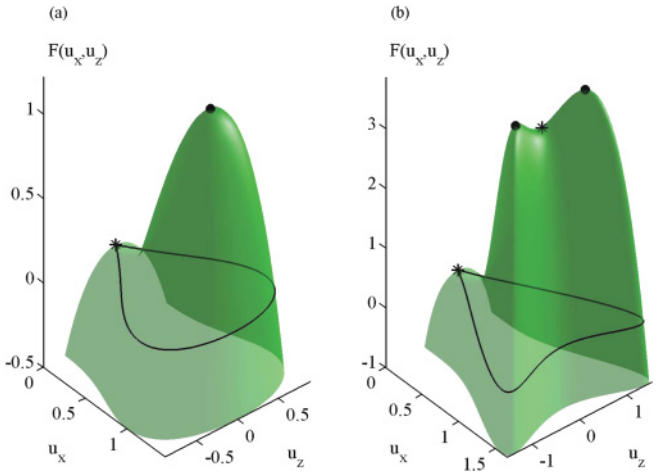

FIG. 2. (Color online) Plots of $F(u_x,u_z)$ evaluated for $\sigma_\epsilon = 1$, $\sigma_\mu = 1$, $u_{x0}^2 = 2$, and (a) $\gamma = 0.5$ and (b) $\gamma = 3$. Black lines correspond to the homoclinic orbits; the stars and circles are located at the saddle points and maxima of $F(u_x,u_z)$, respectively.

in contrast, in the case $\gamma > 1$ and $u_{x0}^2 > \delta$ [see Fig. 2(b)] where

$$\delta(\gamma) = \frac{(\gamma+2)+\sqrt{5\gamma^2+2\gamma}}{2(\gamma^2-1)}, \tag{13}$$

F has two saddle points (located at $(u_x,u_z) = [\sqrt{(\beta^2-1)/(1+\gamma)},0]$ and the origin $(u_x,u_z) = (0,0)$) and two maxima not belonging to the axis $u_z = 0$ [hence characterized by the condition $\epsilon_z^{\rm NL} = 0$; see Eqs. (12)]. From Fig. 2 it is evident that, in the situations considered, the homoclinic (solitonic) orbits make a turn around the maxima of the function $F(u_x,u_z)$ so that the shape of the orbits (and consequently the soliton profiles) depends on the number of maxima enclosed by the homoclinic loop. Therefore, since there are one and two maxima for $|\gamma| < 1$ and $\gamma > 1$ (for $u_{x0}^2 > \delta$), respectively, we conclude that homoclinic orbits undergo a qualitative structural change at $\gamma = 1$. Correspondingly, for $|\gamma| < 1$ homoclinic orbits are simple loops [see Fig. 2(a)] and solitons are bell shaped, whereas for $\gamma > 1$ (for $u_{x0}^2 > \delta$) homoclinic orbits are structured loops [see Fig. 2(b)] and two-peaked solitons occur. In other words (in language closer to nonlinear optics) the two kinds of bright solitons discussed herein are supported by two different self-trapping mechanisms and the nonlinear metamaterials employed in this work provide the additional parameter γ to switch from one mechanism to the other. It is worth noting that the first of Eqs. (12) holds globally for all the maxima considered, whereas the second of Eqs. (12) is fulfilled differently since, for $|\gamma| < 1$ and $\gamma > 1$ (for $u_{x0}^2 > \delta$), maxima occur for $u_z = 0$ and $\epsilon_z^{\rm NL} = 0$, respectively. Therefore, bell-shaped solitons are not constrained by additional specific requirements and actually coincide with the perfect solitons of Ref. [12]. In contrast, two-peaked solitons supported by the self-trapping mechanism considered are due (for $u_{x0}^2 > \delta$) to the existence of off-axis maxima of F corresponding to the condition $\epsilon_z^{\rm NL} = 0$. However, the normalized effective nonlinear permittivity $\epsilon_z^{\rm NL}$ can vanish only if the nonlinear contribution to the polarization $(1-\gamma)u_x^2 + (1+\gamma)u_z^2$ balances exactly the linear part $\sigma_\epsilon = 1$ [see the second of Eqs. (7)]. It is worth repeating that this condition [which is equivalent to Eq. (3)] is realistically achievable solely by means of the nonlinear metamaterials with dielectric permittivity very close to zero that we are considering in this paper.

IV. FLAT-TOP SOLITONS

A second group of bright solitons (see Table I) exists for $u_{x0}^2 < \alpha$ where

$$\alpha(\gamma) = \frac{\sqrt{|\gamma|}-2+\sqrt{5|\gamma|-4\sqrt{|\gamma|}}}{2(|\gamma|-1)(\sqrt{|\gamma|}+1)} \tag{14}$$

in the range $\gamma < -1$ and for $\sigma_\epsilon = -1$ and $\sigma_\mu = -1$ (i.e., for right-handed metamaterials with defocusing nonlinearity $\chi < 0$ or for left-handed metamaterial with focusing nonlinearity $\chi > 0$). In Figs. 3(a) and 3(b) we report the soliton profiles (for various u_{x0}^2) of u_x and u_z, respectively, and in Fig. 3(c) we plot the corresponding normalized Poynting vector S_z/S_0 for $\mathrm{sgn}(\epsilon) = 1$, $\mathrm{sgn}(\mu) = 1$, $\mathrm{sgn}(\chi) = -1$, and $\gamma = -1.5$. In addition, in Figs. 3(d) and 3(e) we report the effective normalized nonlinear dielectric permittivities $\epsilon_x^{\rm NL}(\xi)$ and $\epsilon_z^{\rm NL}(\xi)$, respectively, of Eqs. (7) evaluated for the profiles of $u_x(\xi)$ [Fig. 3(a)] and $u_z(\xi)$ [Fig. 3(b)]. Note that for each $\gamma < -1$, if u_{x0}^2 is very close to α (i.e., for $u_{x0}^2 > 0.99\alpha$), flat-top bright solitons occur since their electric-field x component and Poynting vector profiles are characterized by a flat and sharp core region (where the intensity is almost constant) that abruptly stops being surrounded by lateral regions where the field approximately vanishes. In contrast, for smaller intensities (i.e., for $u_{x0}^2 < 0.99\alpha$) solitons are characterized by a bell-shaped profile. It is worth noting that in the region where the soliton Poynting vector displays the flat-top profile, the

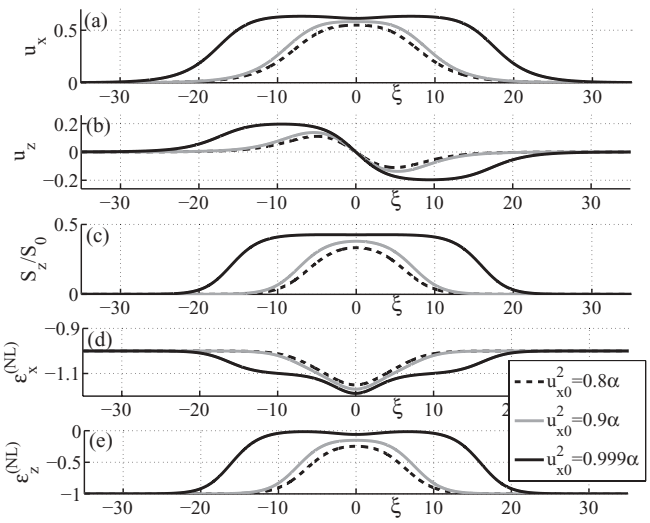

FIG. 3. Profiles of (a) $u_x(\xi)$, (b) $u_z(\xi)$, and (c) the normalized Poynting vector $S_z(\xi)/S_0$ of various (with different u_{x0}^2) bright solitons for $\sigma_\epsilon = -1$, $\sigma_\mu = -1$, $\mathrm{sgn}(\chi) = -1$, and $\gamma = -1.5$. Also shown are the effective normalized nonlinear dielectric permittivities (d) $\epsilon_x^{\rm NL}(\xi)$ and (e) $\epsilon_z^{\rm NL}(\xi)$ of Eqs. (7) evaluated for the profiles of $u_x(\xi)$ [from (a)] and $u_z(\xi)$ [from (b)].

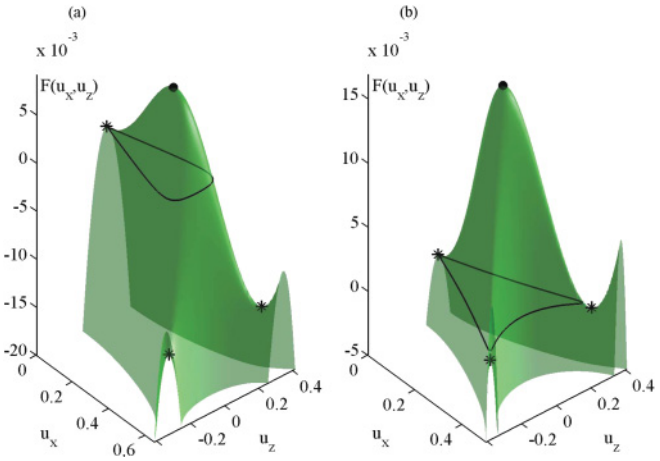

FIG. 4. (Color online) Plots of $F(u_x,u_z)$ evaluated for $\sigma_\epsilon = -1$, $\sigma_\mu = -1$, $\gamma = -7$, and (a) $u_{x0}^2 = 0.8\alpha$ and (b) $u_{x0}^2 = 0.99\alpha$. Black lines correspond to the homoclinic orbits; the stars and circles are located at the saddle points and maxima of $F(u_x,u_z)$, respectively.

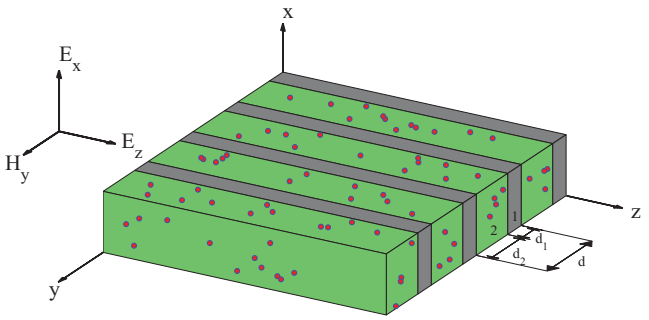

FIG. 5. (Color online) Composite nonlinear metamaterial for achieving $\epsilon \ll 1$ and $\gamma > 1$ or $\gamma < -1$. The layers are staked along the magnetic-field direction of the impinging TM wave. Layers of the first kind are filled with a doped semiconductor (as ZnO:Al or ZnO:Ga) whose doping is tuned to largely reduce the plasma frequency and hence to provide a negative dielectric with small absorption. Layers of the second kind are filled with a nonlinear medium characterized by a molecular orientation Kerr response and hosting dispersed semiconductor quantum dots.

overall normalized dielectric permittivities $\epsilon_x^{\rm NL}(\xi)$ [Fig. 3(d)] and $\epsilon_z^{\rm NL}(\xi)$ [Fig. 3(e)] are significantly different from their linear values [i.e., $\epsilon_x^{\rm NL}(\infty) = \epsilon_z^{\rm NL}(\infty) = \sigma_\epsilon = -1$] so that the solitons considered can be observed only in the extreme nonlinear regime where the nonlinear contribution to the medium polarization is comparable to the linear one.

Even the mechanism leading to the formation of flat-top solitons can be understood by considering the critical point of the first integral F. For $\gamma < -1$, it is simple to prove that the two off-axis critical points (i.e., with $u_z \neq 0$ and satisfying $\epsilon_z^{\rm NL} = 0$) obtained by Eqs. (12) are saddle points of F; this is particularly evident from Figs. 4(a) and 4(b), where we plot such saddle points (marked with stars) together with the first integral F on the phase space (u_x,u_z) for $u_{x0}^2 = 0.8\alpha$ and 0.99α, respectively (for the parameters $\sigma_\epsilon = -1$, $\sigma_\mu = -1$, and $\gamma = -7$). Analogously to the case of the two-peaked solitons discussed above, the off-axis critical points of F have a significant impact on the structure of the homoclinic orbits and, in the case $\gamma < -1$ we are considering, the fact that they are saddle points implies that the homoclinic orbit cannot make a turn around them. Therefore, by varying u_{x0}^2 (for each $\gamma < -1$), the mutual position (and distance) between the homoclinic orbit and the saddle points can be changed (see Fig. 4) to the point that, for u_{x0}^2 very close to α, the homoclinic orbit almost collides with the saddle points. When this happens at the points (u_x,u_z) of the homoclinic orbit that are very close to the saddle points, the right-hand sides of Eqs. (6) are very small (since at the saddle point they vanish exactly) and therefore $du_x/d\xi$ and $du_z/d\xi$ are very small as well, thus explaining the flat-top soliton behavior obtained. In the language of nonlinear optics, we can state that, for $\gamma < -1$, Kerr nonlinearity provides an additional self-trapping mechanism very different from the two mechanisms supporting bell-shaped ($|\gamma| < 1$) and two-peaked ($\gamma > 1$) solitons discussed above. It is worth stressing again that, since the two saddle points occur where the effective nonlinear permittivity vanishes ($\epsilon_z^{\rm NL} = 0$), the overall flat-top soliton phenomenology we discussed can be uniquely observed by means of the extreme nonlinear metamaterials we are considering in this paper.

V. NONLINEAR METAMATERIAL DESIGN AND SOLITON FEASIBILITY

The possibility of observing both two-peaked and flat-top solitons is substantially based on the availability of nonlinear Kerr media characterized by a very small dielectric permittivity and a parameter γ in the ranges $\gamma < -1$ and $\gamma > 1$, respectively. In order to discuss the feasibility of metamaterials exhibiting such unconventional properties, consider the composite structure reported in Fig. 5, which consists of alternating, along the y axis, two kinds of nonmagnetic layers of thicknesses d_1 and d_2, respectively. Here we consider monochromatic radiation whose free-space wavelength is $\lambda = 1550$ nm and whose electromagnetic TM field geometry is also reported in Fig. 5 from which it is evident that such an electromagnetic field experiences an isotropic response. The first kind of layer is filled with a suitable semiconductor that can be doped to lower its plasma frequency to the point that, at the wavelength considered, its dielectric permittivity has a negative real part and a considerably small imaginary part [18] (zinc oxide is a good candidate that can be doped sufficiently high, for example with aluminium or gallium, to satisfy these requirements [19]); in addition, semiconductors are characterized by a standard nonresonant electronic Kerr response (for which $\gamma = 0.5$). Therefore, for the first kind of layer, we choose $\epsilon_1 = -8 + 0.1i$, $\chi_1 = -5 \times 10^{-20}$ m^2/V^2, and $\gamma_1 = 0.5$ [20,21]. The second kind of layer has to be filled with a nonlinear medium whose Kerr mechanism is different from the nonresonant electronic one (otherwise the whole structure would exhibit $\gamma = 0.5$) and it has to host a gain mechanism for compensating losses produced by the semiconductor (negative dielectric) layers of the first kind. Therefore, for the second kind of layer we choose a background medium for which $\epsilon_b = 2.66$, $\chi_b = 3 \times 10^{-20}$ m^2/V^2, and $\gamma_b = 3$ (the nonlinear parameters being

typical of media characterized by a molecular orientation Kerr response [15]), hosting semiconductor nanoparticles (optically pumped quantum dots) for which $\epsilon_{QD} = 11.8 - 5.7i$, $\chi_{QD} = 10^{-20}$ m^2/V^2, and $\gamma_{QD} = 0.5$ (these parameters characterizing suitable InAs/GaAs quantum dots, as discussed in Ref. [22]). In order to obtain the effective electromagnetic linear and nonlinear parameters of the whole structure of Fig. 5, we exploit a two-step homogenization approach [23] where, first, the effective parameters of the second kind of layer are evaluated from the background medium and quantum-dot properties and, second, the effective parameters of the whole structure are obtained from those of the first and second kinds of layers. Layers of the second kind can be homogenized by exploiting the standard Maxwell-Garnett approach (for evaluating the effective linear permittivity) and its nonlinear extension proposed by Sipe and Boyd in Ref. [17] (for deducing the effective nonlinear parameters of the composite) so that, by choosing the macroscopic volume filling fraction of the quantum dots $f = 0.03$, we obtain, for the second kind of layer, $\epsilon_2 = 2.79 - 0.03i$, $\chi_2 = (3.61 \times 10^{-20} - 1.6 \times 10^{-21}i)$ m^2/V^2, and $\gamma_2 = 2.68 + 0.07i$. If the period $d = d_1 + d_2$ (see Fig. 5) is much smaller than the wavelength, effective linear [24] and nonlinear [25] parameters can be introduced to describe the overall layered composite electromagnetic response so that, by choosing $d_1 = 52$ nm and $d_2 = 148$ nm, we obtain $\epsilon = 1.5 \times 10^{-3} + 10^{-4}i$, $\chi = (1.38 \times 10^{-20} - 1.21 \times 10^{-21}i)$ m^2/V^2, and $\gamma = 4.70 + 0.32i$ (where the nonlinear parameters have been evaluated by exploiting the approach of Ref. [8]). Note that $\mathrm{Re}(\epsilon) = 0.0015 \ll 1$, $\mathrm{Re}(\gamma) = 4.70 > 3$ (different from both the standard values of 0, 0.5, and 3 and those achieved in Ref. [17]), and, remarkably, all the imaginary parts can be neglected so that the conditions for observing the two-peaked solitons discussed above are met. It is worth stressing that the fulfillment of all these conditions has been achieved by exploiting both the number of available constituent materials and, most importantly, the freedom of tuning the parameters characterizing the composite (semiconductor doping, nanoparticle size, volume filling fraction, and layer thickness, etc.). Another important remark is related to the fact that the medium tailored above is such that $\mathrm{Im}(\epsilon) \ll \mathrm{Re}(\epsilon)$, $\mathrm{Im}(\chi) \ll \mathrm{Re}(\chi)$, and $\mathrm{Im}(\gamma) \ll \mathrm{Re}(\gamma)$ and these conditions are essential for the proprosed medium to be suitable for observing the theoretical predictions of the soliton obtained for real values of the medium's electromagnetic parameters. Specifically, the small imaginary part of the dielectric permittivity does not severely affect the transverse soliton phenomenology, but is responsible only for a finite soliton propagation length, which can be estimated to be $L = \lambda/2\pi\,\mathrm{Im}(\sqrt{\epsilon}) \simeq 0.2$ mm, which is a macroscopic distance suitable for potential photonic-device applications. A two-peaked soliton, propagating through the medium considered above and characterized by $u_{x0}^2 = 0.5$, has a width of 19.4 μm (coinciding with twice the root of the variance of the spatial intensity profile) and requires the peak intensity 775 MW/cm^2 to be excited, a value that should be compared with the unphysical peak intensity 1.93×10^7 MW/cm^2 that is required for exciting a similar (i.e., with $u_{x0}^2 = 0.5$) two-peaked soliton through carbon disulfide (for which $\epsilon_{CS_2} = 2.65$, $\chi_{CS_2} = 3 \times 10^{-20}$ m^2/V^2, and $\gamma_{CS_2} = 3$). Therefore, the extremely high nonlinear behavior of the two-peaked soliton considered would require, in conventional media, optical intensities so high that their observation would be prevented both because the nonlinear response would depart from the simple Kerr model and, most importantly, because the very high intensity would literally damage the sample.

If in the composite structure discussed above the nonlinear susceptibility of the first kind of layer is changed into $\chi_1 = -2 \times 10^{-19}$ m^2/V^2, by following the two-step homogenization approach described above we obtain, for the overall composite medium, $\epsilon = 1.5 \times 10^{-3} + 1 \times 10^{-4}i$, $\chi = (-2.5 \times 10^{-20} - 1.21 \times 10^{-21}i)$ m^2/V^2, and $\gamma = -1.83 + 0.14i$. Therefore, the dielectric permittivity is very small, the overall nonlinear character is defocusing [since $\mathrm{Re}(\chi) < 0$], and, most importantly, $\mathrm{Re}(\gamma) < -1$, so that all the conditions required for observing flat-top solitons are met. A flat-top soliton propagating through the medium considered and characterized by $u_{x0}^2 = 0.99\alpha(\gamma) = 0.32$ has a width of 80.8 μm (coinciding with twice the root of the variance of the spatial intensity profile) and requires the feasible optical intensity 119 MW/cm^2 to be excited.

In addition to the realistic possibility of synthesizing the epsilon-near-zero nonlinear metamaterials discussed above, the feasibility of the predicted soliton phenomenology is evidently related to the actual efficiency of coupling light from a standard medium (e.g., vacuum) to the composite medium considered. In fact, in the linear regime, the fraction of the incident optical power actually penetrating the epsilon-near-zero material is very small due to the large impedance mismatch between the two media. In order to show that in the extreme nonlinear regime the situation can be very different [10], we have investigated analytically two-peak and flat-top soliton excitation from vacuum. Using the electromagnetic matching conditions at the vacuum-metamaterial interface, we have evaluated the optical field (and its transverse intensity

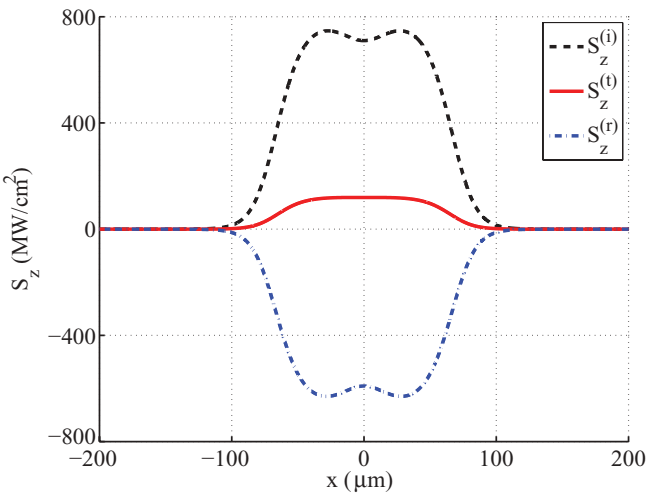

FIG. 6. (Color online) Poynting vector profile $S_z^{(i)}$ of the optical beam impinging from vacuum onto the metamaterial interface and exciting the 119-MW/cm^2 transmitted flat-top soliton, whose Poynting vector profile is $S_z^{(t)}$. $S_z^{(r)}$ is the Poynting vector profile of the vacuum-reflected optical beam. All the intensity profiles are evaluated at the vacuum-metamaterial interface.

profile), which, impinging from vacuum, actually excites a prescribed soliton (see the Appendix). As an example, in Fig. 6 we compare the transmitted Poynting vector profile $S_z^{(t)}$ (solid line) of the 119-MW/cm^2 flat-top soliton considered above with the Poynting vector profiles $S_z^{(i)}$ (dashed line) and $S_z^{(r)}$ (dash-dotted line) of the incident and reflected vacuum beams evaluated at the vacuum-metamaterial interface. Note that the intensity of the transmitted soliton is only one-sixth the top intensity of the incident beam, thus proving that, as a consequence of the impact of the nonlinearity on the overall dielectric response, the optical beam impinging from the vacuum is not fully reflected by the metamaterial interface.

VI. CONCLUSION

In conclusion, we have shown that a medium characterized by the constituent relations of Eqs. (2), with $|\epsilon| \ll 1$ and γ assuming values different from the three available in nature (i.e., 0, 0.5, and 3), is able to support the propagation of two-peaked (for $\gamma > 1$) and flat-top (for $\gamma < -1$) solitons. These two families of electromagnetic (perfect) solitons are supported by two distinct self-trapping mechanisms whose main difference from the standard self-focusing process lies in the availability of critical points where the effective nonlinear response vanishes (a condition made possible by the very small value of the linear permittivity), points able to greatly affect the soliton shape. Since the whole predicted soliton phenomenology is based on unconventional values of γ, we have proposed a realistic and feasible composite metamaterial exhibiting such exotic nonlinear properties. It is worth stressing that, as a consequence of the small value of the linear dielectric permittivity, the intensities required to excite the solitons considered (characterized by highly nonlinear and highly nonparaxial behaviors) are physically accessible. Therefore, the soliton benchmark considered in the present paper allows us to argue that the two self-trapping mechanisms considered can be efficiently exploited to fine-tune the shape of an optical beam, shape control that can even become active by inserting electro-optic- or liquid-crystal-based constituents within the nonlinear metamaterial.

I. APPENDIX: SOLITON EXCITATION FROM VACUUM

In order to investigate the efficiency of soliton excitation at the interface between vacuum ($z < 0$) and the nonlinear epsilon-near-zero medium ($z > 0$), we consider the electromagnetic field at $z = 0^+$ associated with one of the evaluated soliton profile (u_x, u_z), i.e.,

$$E_x^{(t)}(x,0^+) = \sqrt{\left|\frac{\epsilon}{\chi}\right|}u_x(\xi),$$
$$E_z^{(t)}(x,0^+) = i\sqrt{\left|\frac{\epsilon}{\chi}\right|}u_z(\xi),$$
$$H_y^{(t)}(x,0^+) = \mathrm{sgn}(\mu)\sqrt{\left|\frac{\epsilon}{\chi}\right|}\sqrt{\left|\frac{\epsilon_0\epsilon}{\mu_0\mu}\right|}\left(\beta u_x(\xi) - \frac{du_z}{d\xi}(\xi)\right), \tag{A1}$$

where the first two of Eqs. (A1) are obtained from Eqs. (4) and the magnetic field in the third of Eqs. (A1) is obtained from the Maxwell equation $\mathbf{H} = \nabla \times \mathbf{E}/i\omega\mu_0\mu$. Such a soliton field within the medium is produced by an optical beam impinging from vacuum onto the interface $z = 0$ and, at the same time, a reflected optical beam is produced in vacuum as well. Using the standard angular spectrum representation, the electromagnetic fields of the incident (i) and reflected (r) beams are (for $z < 0$)

$$E_x^{(i)}(x,z) = \frac{1}{\omega\epsilon_0}\int_{-\infty}^{+\infty} dk_x e^{i(k_x x + k_z z)} k_z \tilde{H}^{(i)}(k_x),$$
$$E_z^{(i)}(x,z) = -\frac{1}{\omega\epsilon_0}\int_{-\infty}^{+\infty} dk_x e^{i(k_x x + k_z z)} k_x \tilde{H}^{(i)}(k_x), \tag{A2}$$
$$H_y^{(i)}(x,z) = \int_{-\infty}^{+\infty} dk_x e^{i(k_x x + k_z z)} \tilde{H}^{(i)}(k_x)$$

and

$$E_x^{(r)}(x,z) = -\frac{1}{\omega\epsilon_0}\int_{-\infty}^{+\infty} dk_x e^{i(k_x x - k_z z)} k_z \tilde{H}^{(r)}(k_x),$$
$$E_z^{(r)}(x,z) = -\frac{1}{\omega\epsilon_0}\int_{-\infty}^{+\infty} dk_x e^{i(k_x x - k_z z)} k_x \tilde{H}^{(r)}(k_x), \tag{A3}$$
$$H_y^{(r)}(x,z) = \int_{-\infty}^{+\infty} dk_x e^{i(k_x x - k_z z)} \tilde{H}^{(r)}(k_x),$$

respectively, where $k_z = \sqrt{k_0^2 - k_x^2}$ and $H^{(i)}(k_x)$ and $H^{(r)}(k_x)$ are the incident and reflected magnetic-field spatial Fourier spectra, respectively. The continuity of the electric- and magnetic-field tangential components at $z = 0$ yields

$$E_x^{(i)}(x,0^-) + E_x^{(r)}(x,0^-) = E_x^{(t)}(x,0^+),$$
$$H_y^{(i)}(x,0^-) + H_y^{(r)}(x,0^-) = H_y^{(t)}(x,0^+), \tag{A4}$$

which are two independent equations that, after Fourier inversion, can be used to evaluate the angular spectra $H^{(i)}(k_x)$ and $H^{(r)}(k_x)$ for a given soliton profile. Therefore, Eqs. (A2) allow us to evaluate the incident electromagnetic field and, consequently, its intensity profile at $z = 0^-$ given by the longitudinal Poynting vector component $S_z^{(i)} = \frac{1}{2}\mathrm{Re}(E_x^{(i)} H_y^{(i)*})$ (and analogously for the reflected beam).

[1] J. B. Pendry, Phys. Rev. Lett. **85**, 3966 (2000).

[2] N. Fang, H. Lee, C. Sun, and X. Zhang, Science **308**, 534 (2005).

[3] J. B. Pendry, D. Schurig, and D. R. Smith, Science **312**, 1780 (2006).

[4] D. Schurig, J. J. Mock, B. J. Justice, S. A. Cummer, J. B. Pendry, A. F. Starr, and D. R. Smith, Science **314**, 977 (2006).

[5] H. Chen, J. F. O'Hara, A. K. Azad, A. J. Taylor, R. D. Averitt, D. B. Shrekenhame, and W. J. Padilla, Nature Photon. **2**, 295 (2008).

[6] G. L. Fischer, R. W. Boyd, R. J. Gehr, S. A. Jenekhe, J. A. Osaheni, J. E. Sipe, and L. A. Weller-Brophy, Phys. Rev. Lett. **74**, 1871 (1995).
[7] J. B. Pendry, A. J. Holden, D. J. Robbins, and W. J. Stewart, IEEE Trans. Microwave Theory Tech. **47**, 2075 (1999).
[8] A. Ciattoni, C. Rizza, and E. Palange, Phys. Rev. A **81**, 043839 (2010).
[9] A. Ciattoni, C. Rizza, and E. Palange, Opt. Express **18**, 11911 (2010).
[10] A. Ciattoni, C. Rizza, and E. Palange, Opt. Lett. **35**, 2130 (2010).
[11] C. Rizza, A. Ciattoni, and E. Palange, Opt. Commun. **284**, 2573 (2011).
[12] A. Ciattoni, B. Crosignani, P. Di Porto, and A. Yariv, J. Opt. Soc. Am. B **22**, 1384 (2005).
[13] F. Gori, Opt. Commun. **1070**, 335 (1994).
[14] H. Ma, Z. Liu, P. Zhou, X. Wang, Y. Ma, and X. Xu, J. Opt. **12**, 045704 (2010).
[15] R. W. Boyd, *Nonlinear Optics* (Academic, New York, 1994).
[16] M. Silveirinha and N. Engheta, Phys. Rev. Lett. **97**, 157403 (2006).
[17] J. E. Sipe and R. W. Boyd, Phys. Rev. A **46**, 1614 (1992).
[18] R. G. Gordon, Mater. Res. Soc. Bull. **25**, 52 (2000).
[19] M. Hiramatsu, K. Imaeda, N. Horio, and M. Nawata, J. Vac. Sci. Technol. A **16**, 669 (1998).
[20] Sofiani, B. Sahraoui, M. Addou, R. Adhiri, M. A. Lamrani, L. Dghoughi, N. Fellahi, B. Derkowska, and W. Bala, J. Appl. Phys. **101**, 063104 (2007).
[21] B. Kulyk, B. Sahraoui, V. Figa, B. Turko, V. Rudyk, and V. Kapustianyk, J. Alloys Compd. **481**, 819 (2009).
[22] A. Bratkovsky, E. Ponizovskaya, S. Wang, P. Holmström, L. Thylén, Y. Fu, and H. Gren, Appl. Phys. Lett. **93**, 193106 (2008).
[23] A. I. Cabuz, D. Felbacq, and D. Cassagne, Phys. Rev. Lett. **98**, 037403 (2007).
[24] W. Cai and V. Shalaev, *Optical Metamaterials: Fundamentals and Applications* (Springer, Dordrecht, 2010).
[25] R. W. Boyd and J. E. Sipe, J. Opt. Soc. Am. B **11**, 297 (1994).